

Increased bandwidth of NbN phonon cooled hot electron bolometer mixers

M. Hajenius^{1,2}, J.J.A. Baselmans², J.R. Gao^{1,2}, T.M. Klapwijk¹, P.A.J. de Korte²,
B. Voronov³ and G. Gol'tsman³

¹*Kavli institute of Nanoscience, Delft University of Technology, Lorentzweg 1,
2628 CJ Delft, The Netherlands.*

²*SRON National Institute for Space Research, Sorbonnelaan 2, 3584 CA Utrecht,
The Netherlands*

³*Moscow State Pedagogical University, Moscow 119435, Russia.*

Abstract

We study experimentally the IF gain bandwidth of NbN phonon-cooled hot-electron-bolometer (HEB) mixers for a set of devices with different contact structures but an identical NbN film. We observe that the IF bandwidth depends strongly on the exact contact structure and find an IF gain bandwidth of 6 GHz for a device with an additional superconducting layer (NbTiN) in between the active NbN film and the gold contact to the antenna. These results contradict the common opinion that the IF bandwidth is determined by the phonon-escape time between the NbN film and the substrate. Hence we calculate the IF gain bandwidth of a superconducting film using a two-temperature model. We find that the bandwidth increases strongly with operating temperature and is not limited by the phonon escape time. This is because of strong temperature dependence of the phonon specific heat in the NbN film.

1. Introduction

Phonon cooled Superconducting Hot Electron Bolometer (HEB) mixers are the most sensitive heterodyne receivers for frequencies above 1 THz and are therefore expected to play a key role in future atmospheric and space borne missions. However, the IF Gain Bandwidth at the bias point that gives the maximum sensitivity is of the order of ~ 3 GHz, which is disappointingly low for many applications [1].

The maximum bandwidth, set by thermal relaxation processes in the bolometer, is believed to be limited by the phonon escape time and not by the electron-phonon interaction time. The phonon escape time is determined by the NbN film thickness and the film-substrate interface. For that reason higher bandwidths were mainly achieved by NbN thin film development [2, 3].

In contrast we investigate the bandwidth for devices with different types of contacts between the Au antenna and the active NbN film. We find that the IF bandwidth at the optimum operating point increases to 6 GHz if we modify the conventional contact structure by sputter cleaning of the NbN surface and adding a superconducting layer (NbTiN) in between the antenna and NbN film. For a HEB, in which the NbN film is not cleaned and no superconducting interlayer is used, we find a bandwidth of 2 GHz. The processing of the latter contacts is similar to that reported by others [4-6].

We will first introduce the devices with different contacts and then describe the IF bandwidth measurement setup and results. Subsequently we use the Perrin and Vanneste two-temperature model [7, 8] to understand the observed high bandwidth.

2. Devices with different contacts.

The device geometry and contacts are illustrated in Fig. 1. Table 1 summarizes the parameters of the contact types. Devices of type “I” have a conventional contact structure similar to the ones reported in Refs. [4-6]. No cleaning of the contact is performed except for the 6 seconds O₂ plasma etch to remove resist remnants prior to the contact deposition. For type “II” and “III” additional physical etch using Ar⁺ is performed to clean the NbN surface prior to the *in-situ* deposition of the contact pads. The rest of the device fabrication is identical for all devices and similar to the HEB mixer fabrication process used by others. All devices are identical in dimensions with a bridge width of 4 μm and length of ~ 0.4 μm and all are using parts of the same 3.5 nm thick NbN film with a T_c of ~ 10 K on a (single) Si substrate. The details of device characteristics and processing can be found elsewhere [9].

The typical uncorrected DSB noise temperatures at 2.5 THz for the different device types are: T_{N,DSB,I} = 2200 K, T_{N,DSB,II} = 1300 K and T_{N,DSB,III} = 950 K [10].

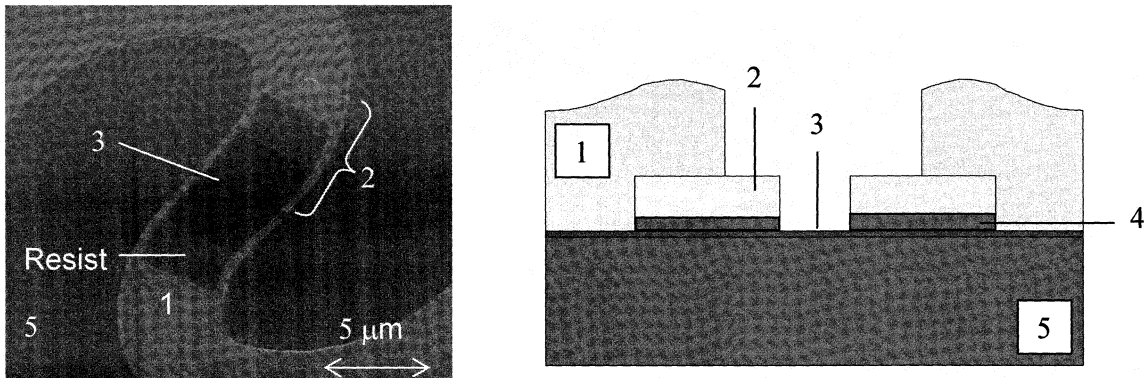


Figure 1. Spiral antenna coupled NbN HEB devices. On the left a SEM picture of the top view of a device and on the right a cross section of the device. “1” indicates the Au spiral antenna structure which is ~ 150 nm thick; “2” the Au layer on the contact pads; “3” the superconducting NbN film, which extends underneath the contact layer/antenna; “4” the intermediate layer between the Au and the NbN film; “5” the Si substrate.

Table 1: Device contact parameters. In all cases a 6 seconds ex-situ O₂ plasma etch is included prior to the contact deposition.

Contact Type	Contact-NbN interface	Contact material
I	No additional cleaning	5 nm Ti + 65 nm Au (Conventional process)
II	15 sec Argon etch	5 nm Nb + 45 nm Au (in situ)
III	15 sec Argon etch	10 nm NbTiN + 40 nm Au (in situ)

3. IF gain bandwidth measurement setup.

The IF gain bandwidth is measured using the setup described in Fig. 2. As a signal source we use a carcinotron with a doubler at a fixed frequency of 600 GHz. The signal is combined with that of a BWO as variable LO source by means of a 60 μm Mylar beam splitter. The cryostat has a 0.9 mm HDPE window and 2 Zytel G104 heat filters. The beam is focused on the device by a hyperhemispherical Si lens. The device is DC biased using a bias T. The IF signal goes through an attenuator before it is fed to a Miteq 0.1 - 8 GHz cryogenic amplifier at 4.2 K with a noise temperature of about 100 K and 30 dB Gain. At room temperature the signal is further amplified and

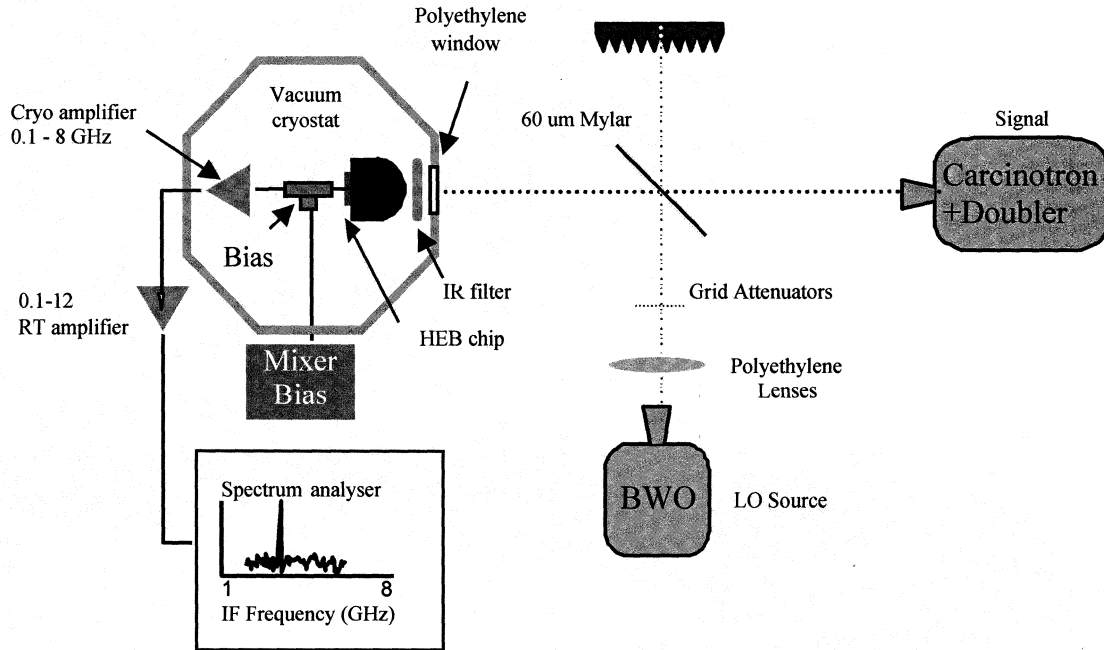


Fig. 2: Measurement setup used to determine the IF gain bandwidth. Essential elements consist of the Signal and LO, which are combined in the beam splitter. This signal is then fed through the cryostat window and heat filter to a lens and focused on the device. The device is biased with a DC voltage bias via the bias T. The resulting signal is subsequently amplified and read out using a spectrum analyzer.

measured using a spectrum analyzer. The amplitude of the IF signal is recorded for different LO frequencies at a fixed signal frequency and care is taken to maintain a constant pumping level of the mixer by monitoring the bias current. The bandwidth is defined as the frequency at which the gain has dropped -3 dB.

The upper frequency limit of our IF chain is measured to be 6 GHz using a SIS junction as a calibrated (shot) noise source. We measure the bandwidth at two bias points: low bias and high bias. The optimum bias point that yields the lowest $T_{N,DSB}$ is called “low bias”. We note that the noise temperature is bias dependent and increases at higher bias voltages. The DC voltage for “high bias” (also listed in table 2) is chosen such that $T_{N,DSB}$ is twice the value at optimum bias. The “low bias” point is close to 0.8 mV for all devices. The measurements are given in Fig. 3 and are summarized in table 2.

4. IF gain bandwidth results for different contacts.

Focusing on the bandwidth at optimal bias point, we find for type I an IF gain bandwidth of 2 GHz, shown in Fig. 3 to the left. This is in line with values reported earlier for similar HEB devices [3-5]. Type II shows a higher bandwidth of 3 GHz (not shown in the figure). The highest bandwidth of 6 GHz is measured for the type III contact, shown in Fig. 3 to the right. Table 2 summarizes the measured bandwidths for all device types.

These results show a clear dependence of the bandwidth on the exact contact structure. The largest difference is found between type I and type III devices. It cannot be explained by a difference in film properties such as phonon escape time since all devices are made from a single wafer. It also cannot be attributed to the out-

diffusion of hot electrons due to the improved contact structure since the latter can not contribute more than 0.5 GHz in IF bandwidth. It is worthwhile to mention that the higher IF bandwidth in type III device is consistent with the estimated LO power. The type III device needs 67 % more LO power than the type I device. This indicates stronger phonon cooling for type III devices. Moreover, the measured value of 6 GHz is higher than the maximum bandwidth of 4.5 GHz for a 3.5 nm NbN film on a Si substrate anticipated by Ref. [3].

We now turn to the bandwidth at high bias. For type I devices we observe that the bandwidth increases to 5 GHz for high bias. This is similar to the previously observed bias dependence of the IF bandwidth for similar devices [2, 5]. Note that for device type III hardly any bias dependence is present.

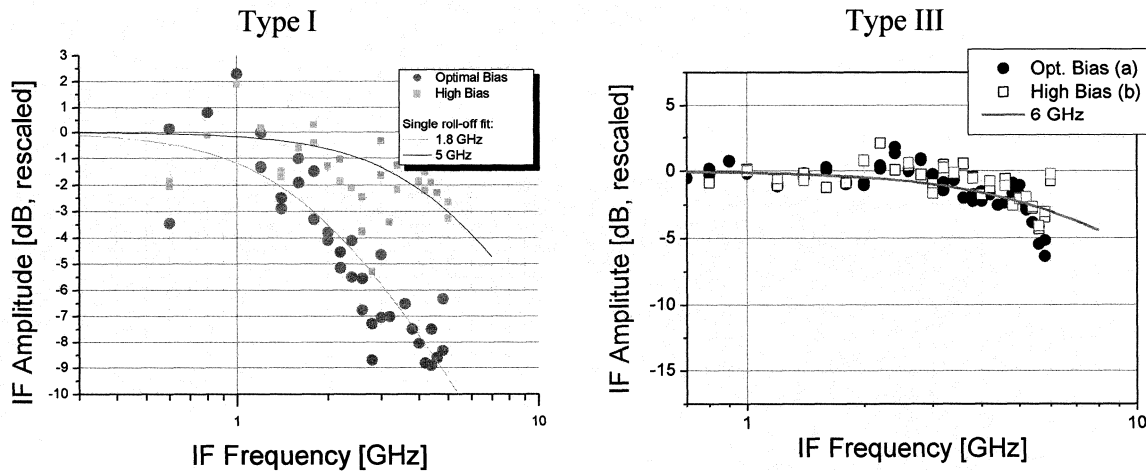


Fig 3: Measured IF amplitude (Relative IF gain). To the left the results for device type I are shown. To the right the results for type III. In both figures the low bias (dots) and high bias (squares) are plotted. The spreading in the data leads to an estimated uncertainty of 1 GHz. The IF bandwidth is defined as the frequency at which the relative IF amplitude is decreased by 3 dB.

Table 2. Measured IF gain bandwidths at 600 GHz of all device types as described in table 1. The IF gain bandwidth is given for both low and high bias points.

Contact Type	IF Gain Bandwidth at low bias	IF Gain Bandwidth at high bias
I	2 GHz	5 GHz
II	3 GHz	5 GHz
III	6 GHz	6 GHz

5. Calculated IF gain bandwidth by Perrin and Vanneste model

Motivated by these experimental results, we have calculated the thermal time constant and thus the IF bandwidth of an irradiated superconducting film by using the two-temperature model proposed by Perrin and Vanneste [7, 8]. Such calculations, also used previously, are believed to provide a guideline for explaining the observed gain bandwidth and to suggest possible further improvement of the bandwidth.

The modeling closely follows the original derivation by Perrin and Vanneste. The results of the model calculations are shown in Fig. 4. Details will be published elsewhere [11].

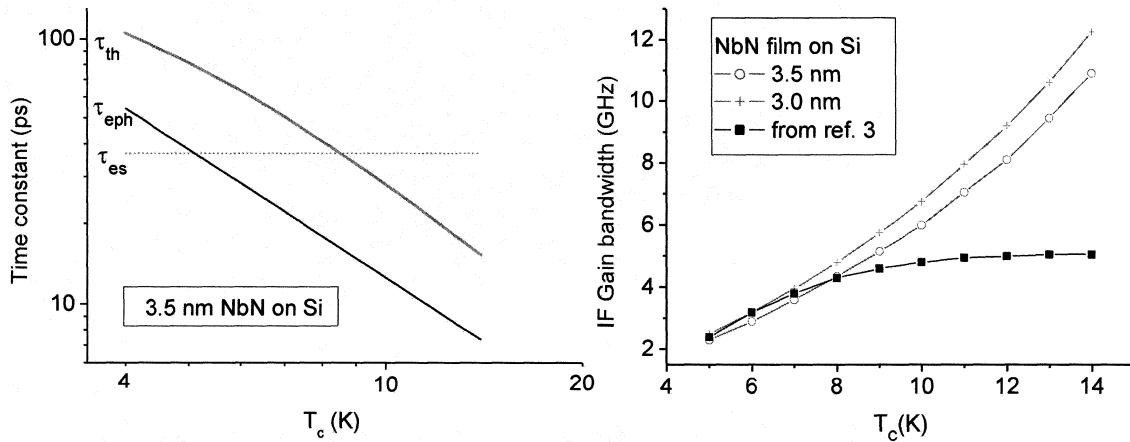


Fig. 4. To the left the dependence of the τ_{es} , the phonon escape time, the τ_{eph} electron phonon relaxation time and the total effective time constant as a function of critical temperature. To the right the IF gain bandwidth as a function of the critical temperature of the film are shown. The black line indicates result of the calculation in Ref. [3]. The crosses give the calculation for a 3 nm NbN film on Si and the connected open circles the calculation for a 3.5 nm NbN film.

In the left graph of Fig. 4 we see the thermal time constant as a function of T_c , the effective temperature for both electrons and phonons, of the devices. Although the phonon escape time is independent of temperature, the thermal time constant still decreases strongly with increasing temperature and becomes significantly shorter than the escape time. Similarly, in the right plot of Fig. 4, we see that the bandwidth increases strongly with temperature, in contrast to the result reported in Ref. [3] in which the bandwidth saturates due to the phonon escape time. Our calculation predicts an IF gain bandwidth of 6 GHz for a 3.5 nm thick NbN film and a T_c of 10 K.

For clarity we like to point out the difference with the modeling in Ref. [3]. Although largely identical, our calculation includes the temperature dependence of the specific heats of both electrons and phonons. Assuming a normal metal, the ratio of the electron heat capacity [12] over the phonon heat capacity [13, 14] rapidly decreases with increasing electron temperature as shown in Fig. 5. Although the escape time for phonons remains constant with increasing temperature, they carry more heat due to their increase of heat capacity, thereby reducing the effective thermal time constant. In the extreme limit where $C_e/C_p \rightarrow 0$, the phonons act as an ideal thermal bath despite of a finite phonon escape time.

To show that the phonon escape time still plays an important role we compare the calculations for a 3.0 with a 3.5 nm NbN film in Fig. 4. The reduction in escape time due to the decrease in thickness corresponds to a significant increase in bandwidth of up to 1 GHz.

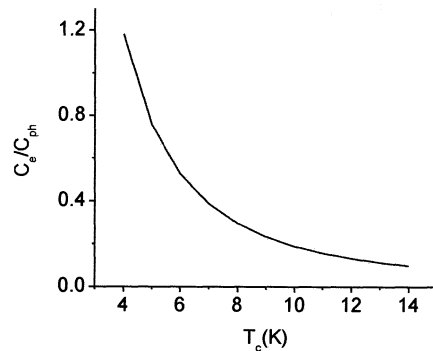


Fig. 5. The ratio of electron heat capacity C_e over the phonon heat capacity C_{ph} as a function of critical temperature. The metal is assumed to be in the normal state and we assume $T_e = T_{ph} = T_c$.

6. Conclusions

In conclusion we have found that the IF bandwidth strongly depends on the HEB contact structure. The improved contacts result not only in improved noise temperatures but also in an enhanced bandwidth. Revisiting the two temperature model of Perrin and Vanneste leads to the result that the calculated gain bandwidth increases strongly with the T_c of superconducting NbN film. The model predicts that a higher electron temperature leads to larger IF bandwidths. The calculation using 3.5 nm and a T_c of 10 K yields the maximum IF bandwidth of 6 GHz, which is consistent with the measured data. However, how the contact structures influence the IF bandwidth remains to be explained. Likely, the contact structures impose a different temperature profile on the NbN bridge, which changes the thermal time. As a by-product of our analysis based on the two temperature model we found the attractive approach to further enlarge the IF bandwidth by increasing the T_c .

Acknowledgments

We wish to thank Willem Jan Vreeling for his skillful assistance during the bandwidth measurements. This work is supported partly by the European Space Agency (ESA) under Contract No. 11653/95/NL/PB.

References

1. Herschel home Page at ESA:<http://astro.estec.esa.nl/SA-general/Projects/First/first.html>.
2. Yuri B. Vachtomin et al. 13th Int. Symp. on Space THz. Techn., Harvard University, Cambridge, MA, May 26-28, 259 (2002)
3. S. Cherednichenko, P. Khosropanah, E. Kollberg, M. Kroug, H. Merkel, Physica C 372-376, 407 (2002)
4. S. Miki, Y. Uzawa, A. Kawakami, Z. Wang, IEEE Trans. On Appl. Supercon. 11 (1), 175 (2001)
5. Matthias Kroug, "NbN Hot Electron Bolometric Mixers for a Quasi-Optical THz Receiver". Ph.D Thesis, Chalmers University of Technology, Goteborg, Sweden (2001).
6. A.D. Semenov, H.-W. Huebers, J. Schubert, G.N. Gol'tsman, A.I. Elantiev, B.M. Voronov, E.M. Gershenzon, J. Appl. Phys. 88, 6758 (2000).
7. N. Perrin and C. Vanneste, "Response of superconducting films to a periodic optical irradiation", Phys. Rev. B 28, 5150, 1983.
8. N. Perrin and C. Vanneste, "Dynamic behavior of a superconductor under time dependent external excitation", J. Physique. 48, 1311 (1987);
9. M. Hajenius, J. J. A. Baselmans, J. R. Gao, T. M. Klapwijk, P. A. J. de Korte, B. Voronov and G. Gol'tsman "Low Noise NbN superconducting Hot Electron Bolometer mixers at 1.9 and 2.5 THz." Supercond. Sci. Technol. 17 (2004) S224–S228
10. J.J.A. Baselmans, M. Hajenius, J.R. Gao, T.M. Klapwijk, P.A.J. de Korte, B. Voronov and G. Gol'tsman, "Doubling of sensitivity and bandwidth in phonon cooled hot electron bolometer mixers", Applied. Phys. Letters, 84, 1958 (2004).
11. J.R. Gao, J.J.A. Baselmans, M. Hajenius, T.M. Klapwijk, and P.A.J. de Korte, Increased Gain Bandwidth of NbN Hot Electron Bolometer Mixers by Raising the Critical Temperature, (in preparation).
12. Ashcroft and Mermin, Solid State Physics, 1979.
13. A.D. Semenov, R. S. Nebosis, Yu. P. Gousev, M. A. Heusinger, and K. F. Renk, "Analysis of the nonequilibrium photoresponse of superconducting films to pulsed radiation by use of a two-temperature model", Phys. Rev. B 52, 581 (1995).
14. S. Cherednichenko, P. Yagoubov, K. Il'in, G. Gol'tsman and E. Gershenzon, "Large bandwidth of NbN phonon cooled hot-electron bolometer mixers on sapphire substrates", Proc. 8th Int. Symp. on Space Terahertz Technology, Cambridge, MA, 245, 1997.